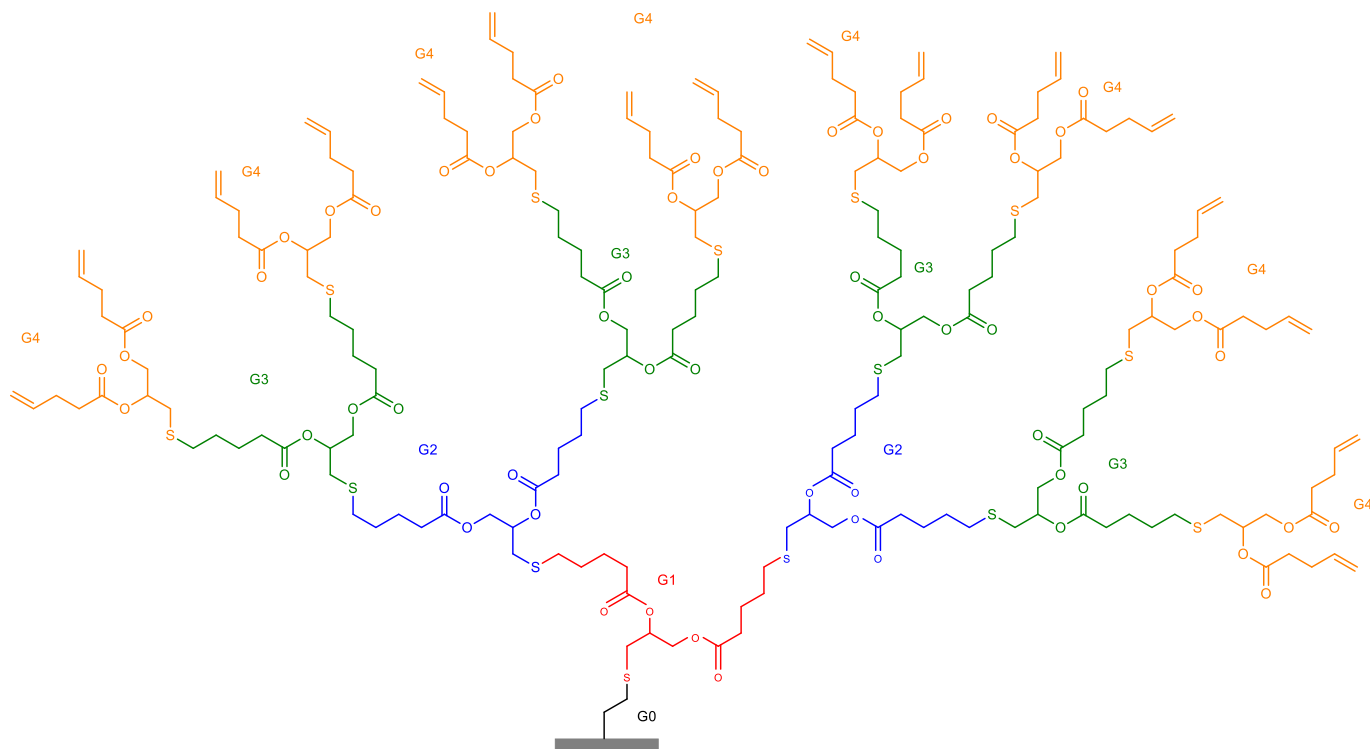


Supplementary Information for

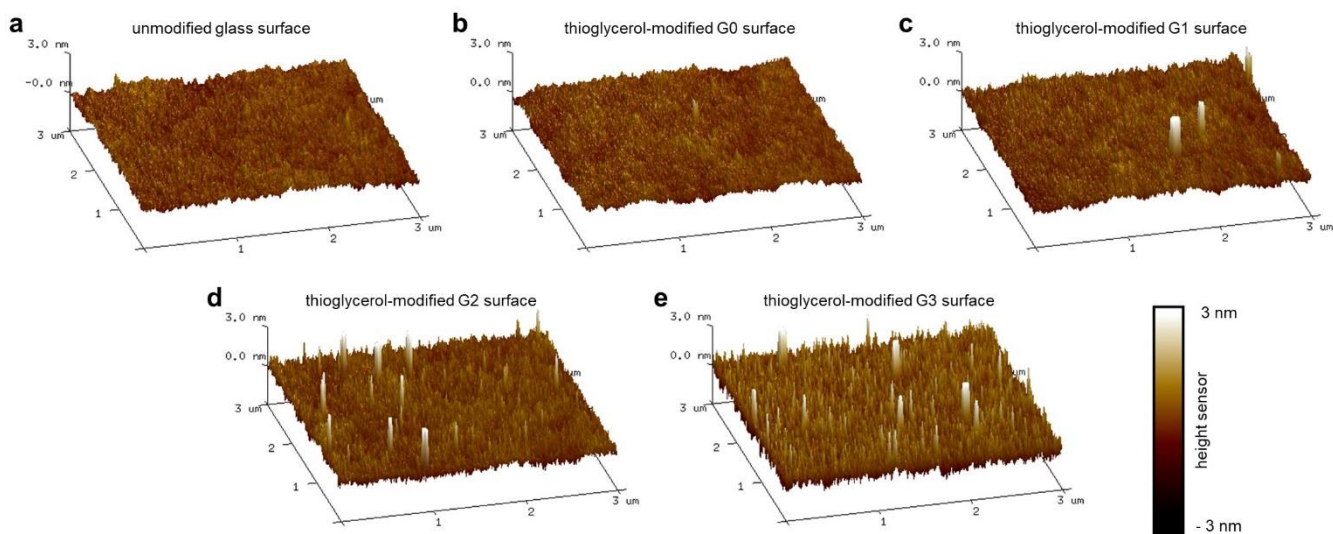
**A combined high-throughput and high-content platform for unified on-chip synthesis, characterization and biological screening**

Benz et al.

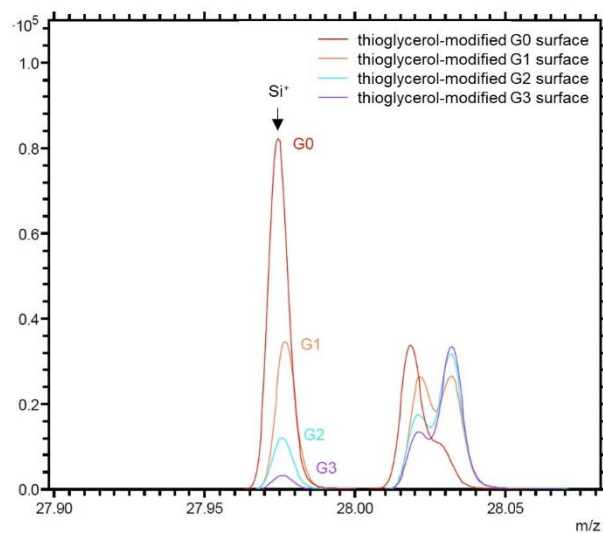
## Supplementary Figures



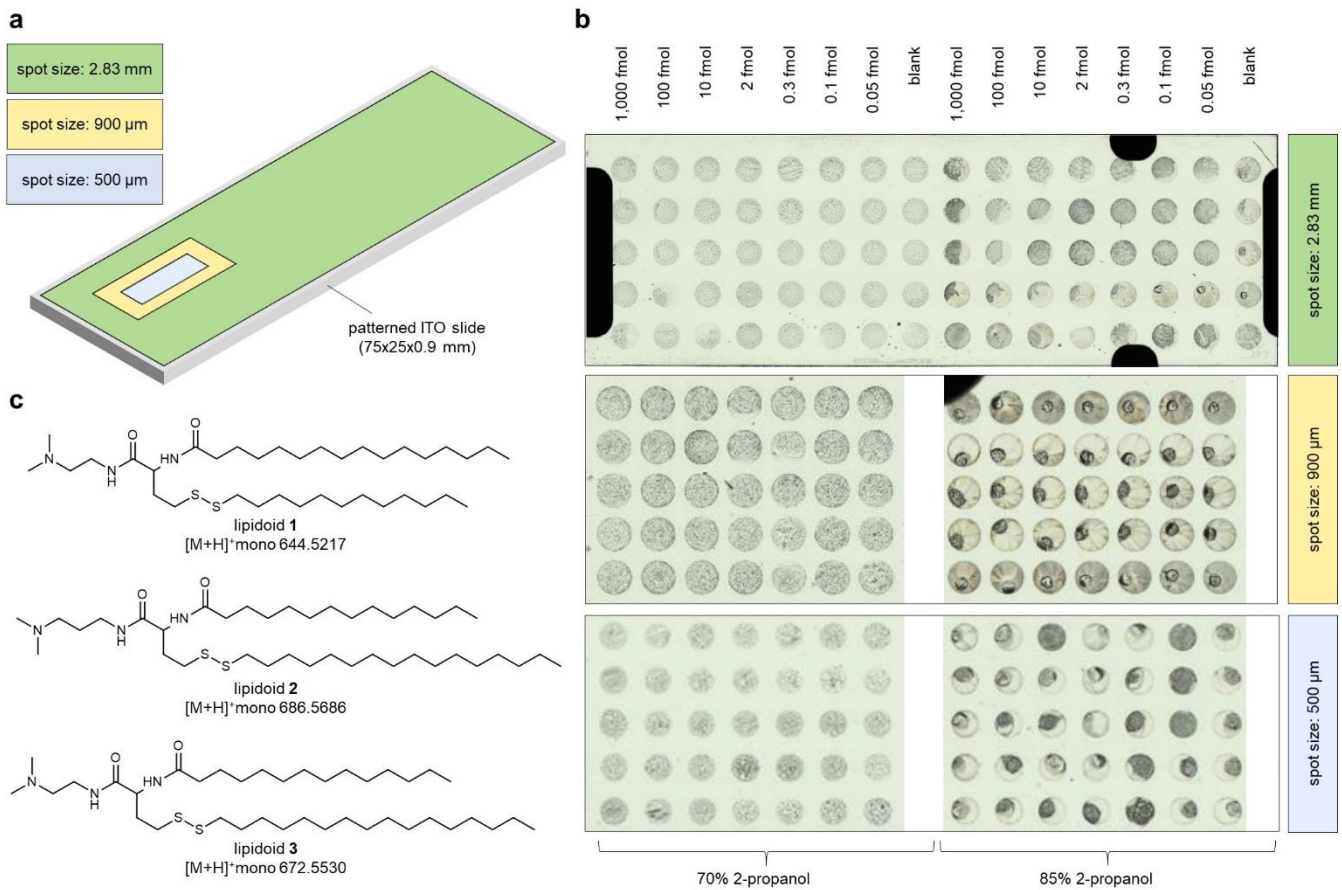
Supplementary Figure 1 | Chemical structure of a surface-grafted G4 dendrimer.



Supplementary Figure 2 | Atomic force microscopy (AFM) surface characterization. AFM image of an (a) unmodified, (b) thioglycerol-modified G0, (c) G1, (d) G2, and (e) G3 surface measured in non-contact tapping mode in air. Field-of-view: 3 x 3 μm<sup>2</sup>.

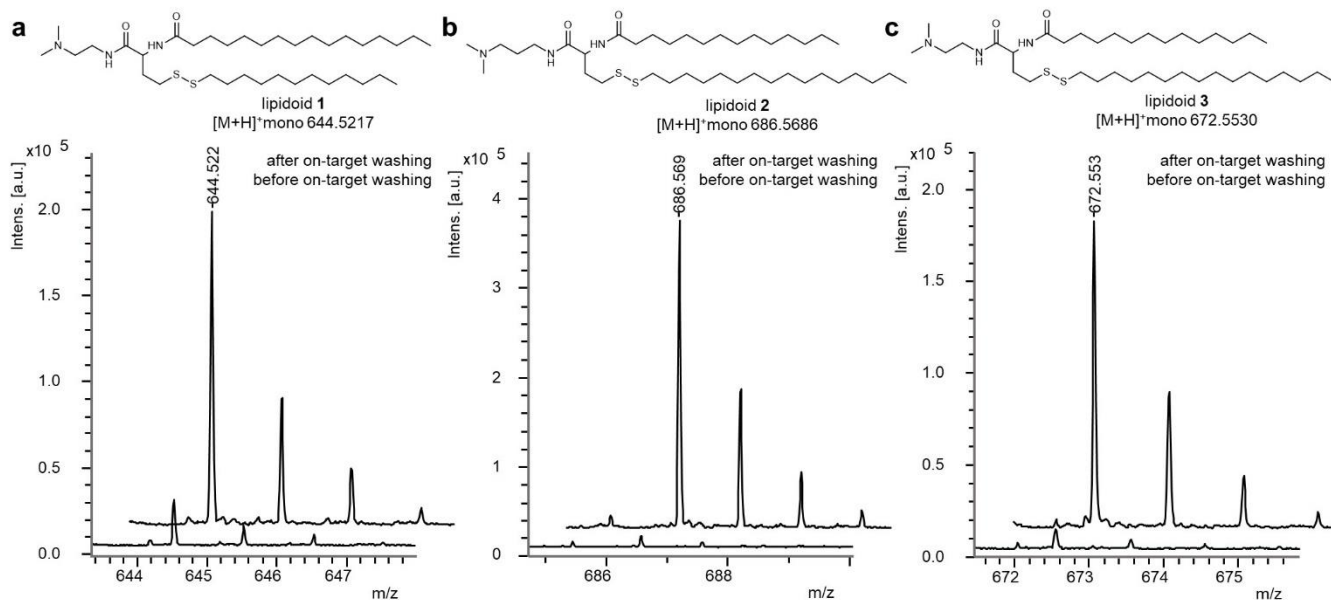


**Supplementary Figure 3 | Time-of-flight secondary ion mass spectrometry (ToF-SIMS) surface characterization.** ToF-SIMS results comparing the Si<sup>+</sup> signal intensity in positive polarity mode of thioglycerol-modified G0-3 surfaces. Source data are provided as a Source Data file.

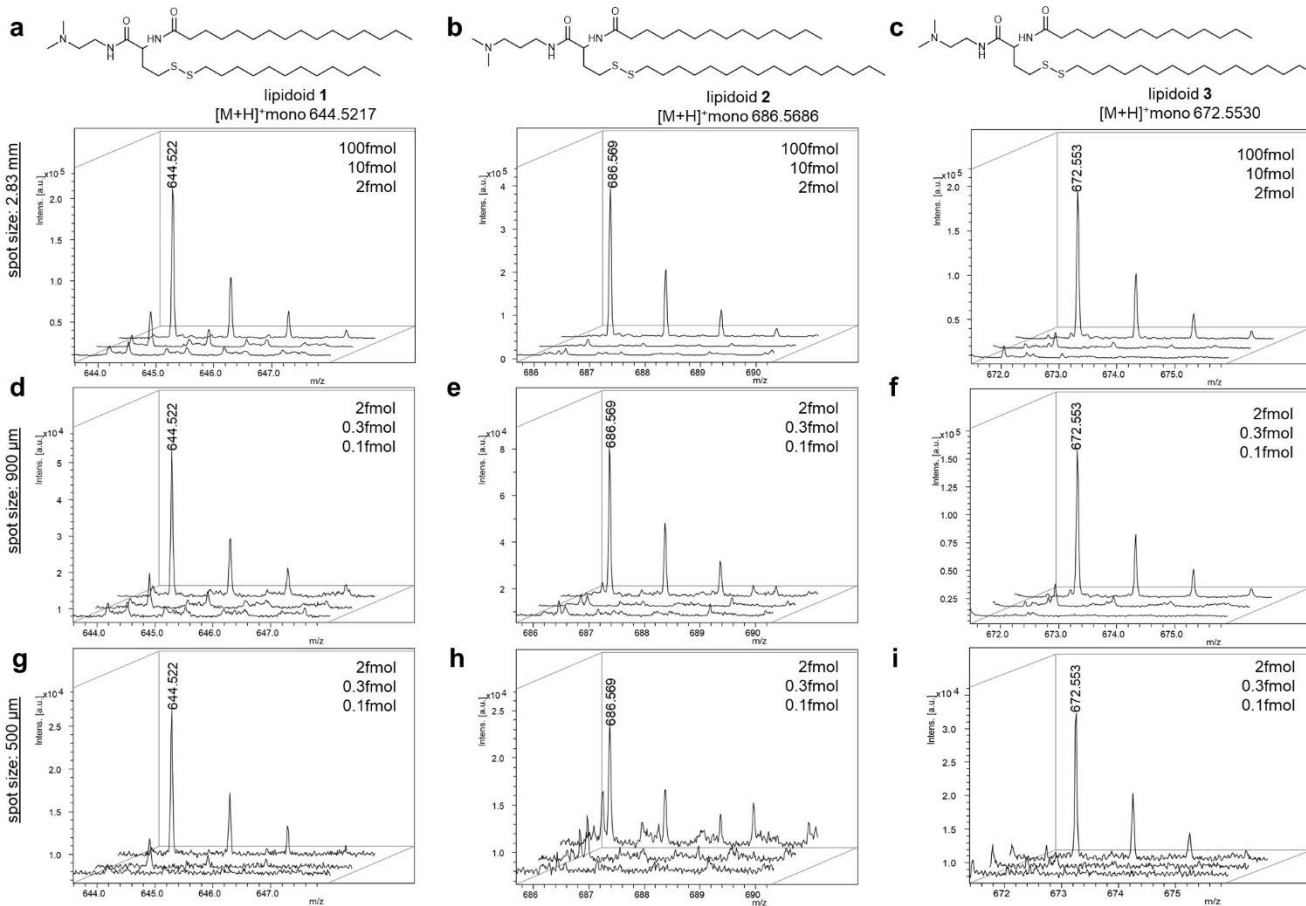


**Supplementary Figure 4 | On-chip matrix-assisted laser desorption / ionization mass spectrometry (MALDI-TOF MS).**

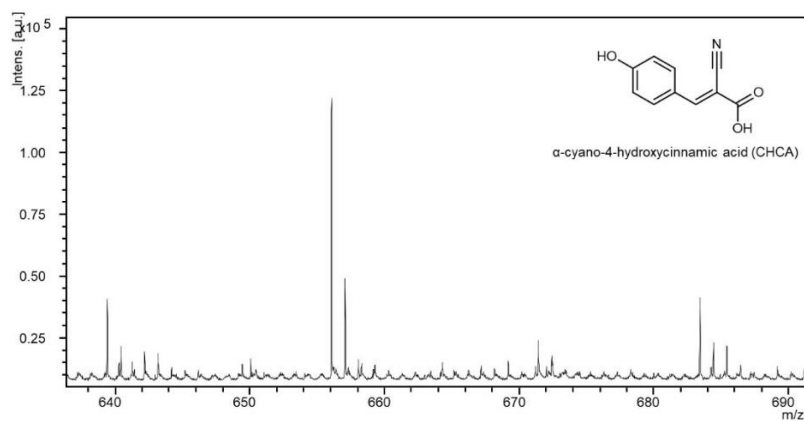
(a) Schematically comparing the required surface area on a omniphilic-omniphobic patterned ITO slide for applying lipidoid **1** in seven different concentrations, each in five replications, and 2x five blank spots (CHCA matrix without sample) on 2.83 mm (spot width: 1.67 mm), 900 μm (spot width: 225 μm) and 500 μm (spot width: 250 μm) round spots. (b) Microscopy images of omniphilic-omniphobic patterned ITO slides with different spot sizes (2.83 mm, 900 μm and 500 μm round spots) containing dried lipidoid **1** in different amounts of substance per spot (1,000, 100, 10, 2, 0.3, 0.1 and 0.05 fmol). Matrix solution was applied using 70 and 85% 2-propanol. (c) Chemical structure of lipidoid **1**, **2** and **3**.



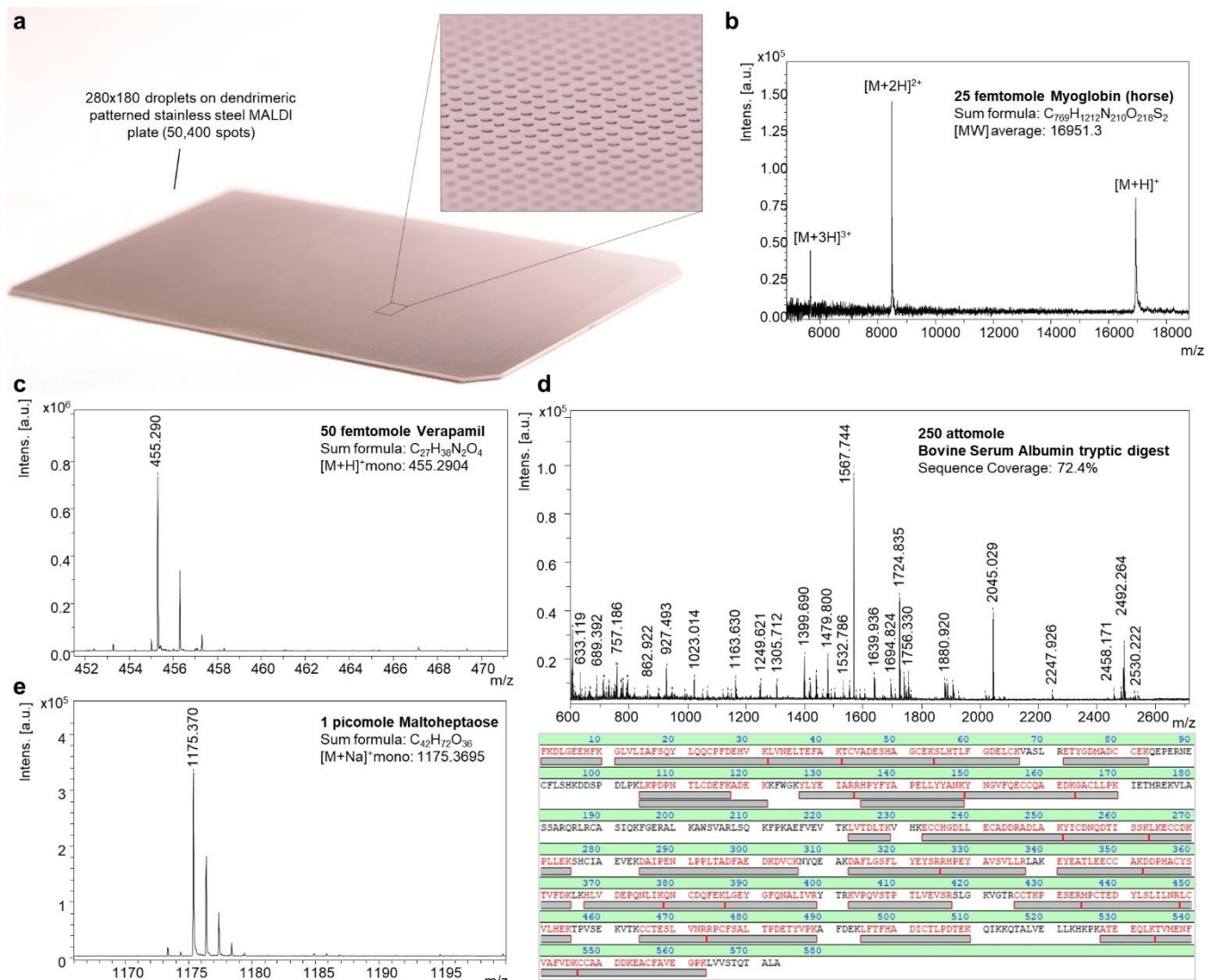
**Supplementary Figure 5 | Effect of on-target washing on MALDI-TOF MS sensitivity.** MS spectra of (a) lipidoid 1 ([M+H]<sup>+</sup>mono: 644.5217), (b) lipidoid 2 ([M+H]<sup>+</sup>mono: 686.5686) and (c) lipidoid 3 ([M+H]<sup>+</sup>mono: 672.5530) before and after on-target washing. Source data are provided as a Source Data file.



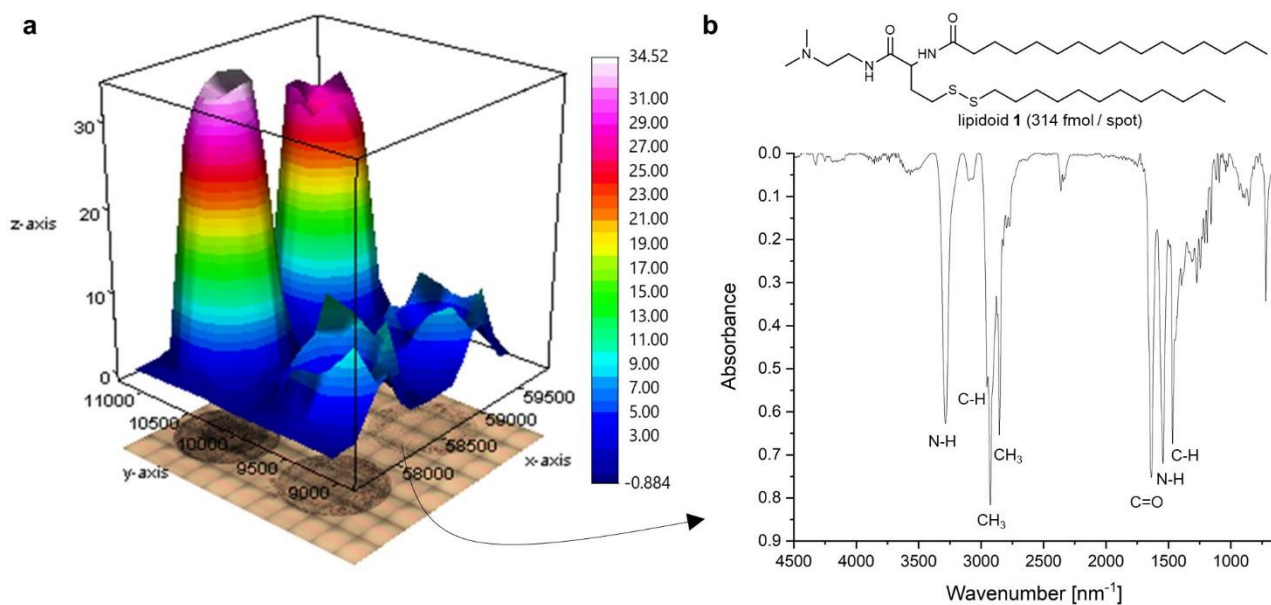
**Supplementary Figure 6 | Sensitivity limitation of on-chip MALDI-TOF MS.** MS spectra of lipidoid 1, 2 and 3 of (a-c) 100, 10 and 2 fmol per 2.83 mm spot, (d-f) 2, 0.3 and 0.1 fmol per 900  $\mu\text{m}$  spot, and (g-i) 2, 0.3 and 0.1 fmol per 500  $\mu\text{m}$  spot. Source data are provided as a Source Data file.



**Supplementary Figure 7 | MALDI-TOF MS spectrum of  $\alpha$ -cyano-4-hydroxycinnamic acid (CHCA) measured on-chip.** Source data are provided as a Source Data file.

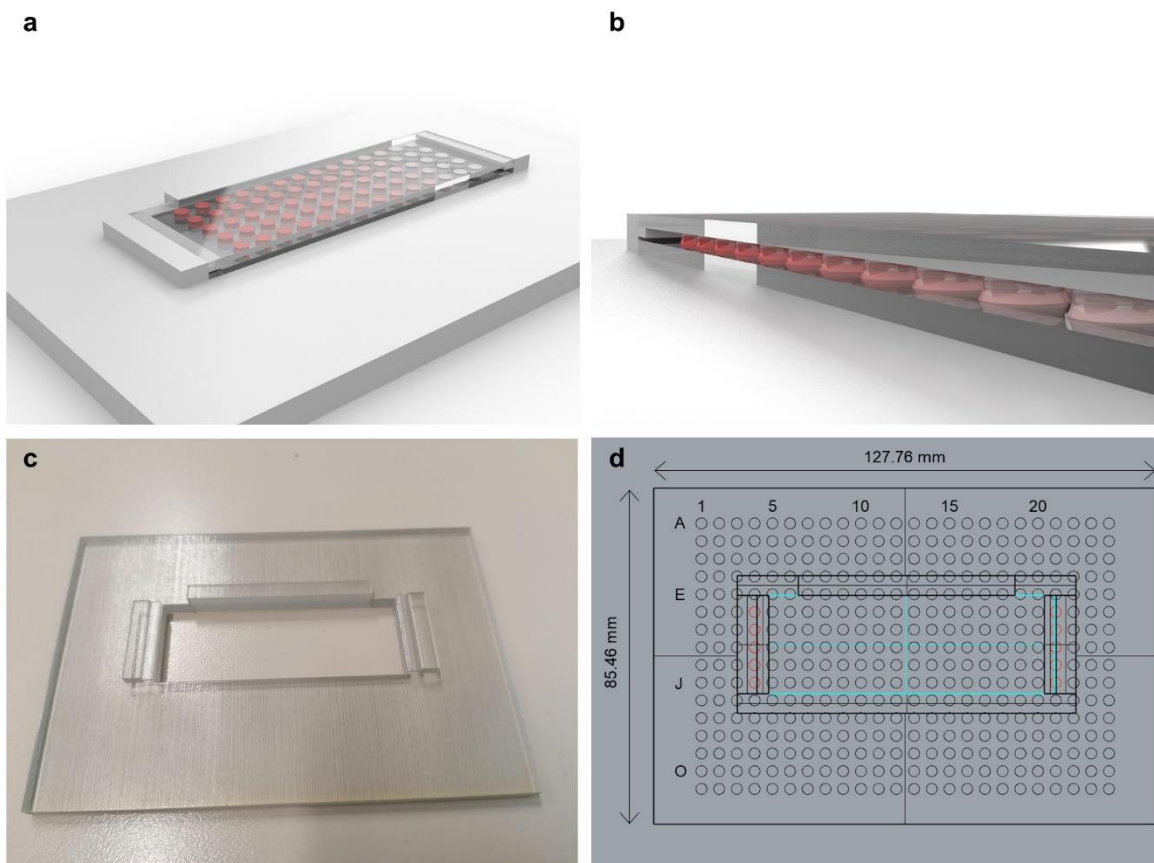


**Supplementary Figure 8 | MALDI-TOF MS on an omniphilic-omniphobic patterned stainless steel plate.** (a) Photograph of a dendrimer-modified and patterned stainless steel plate of microtiter plate size presenting 50,400 individual droplets. Spot size:  $330 \times 330 \mu\text{m}^2$ ; spot distance:  $60 \mu\text{m}$ ; solvent: DMSO. Mass spectra measured on patterned stainless steel plate of (b) 25 femtomole myoglobin, (c) 50 femtomole Verapamil, (d) 250 attomole tryptic digested bovine albumin and (e) 1 picomole maltoheptaose.

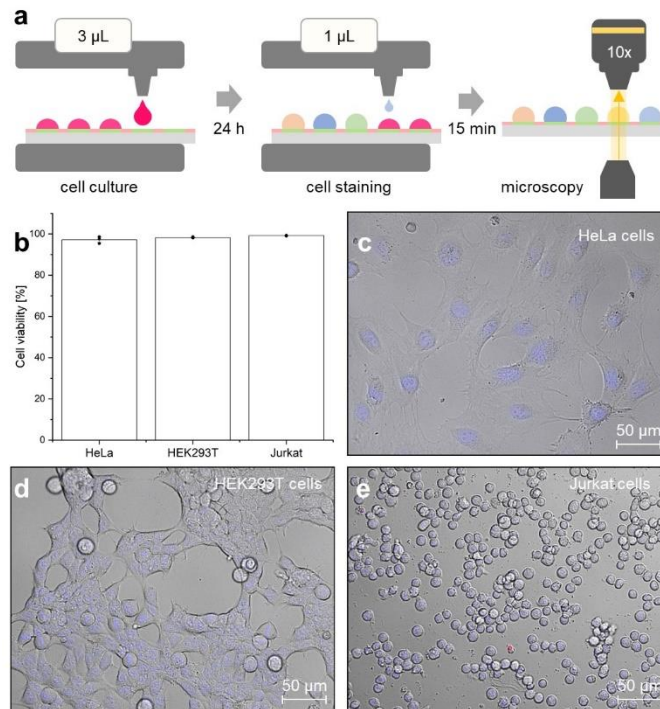


**Supplementary Figure 9 | On-chip characterization by IR spectroscopy. (a)** IR imaging of lipidoid **1** applied in different concentrations on an omniphilic-omniphobic patterned ITO surface. Color scale: Absorbance [a.u.]. **(b)** Corresponding on-chip measured IR spectrum of 314 fmol of lipidoid **1**. Source data are provided as a Source Data file.

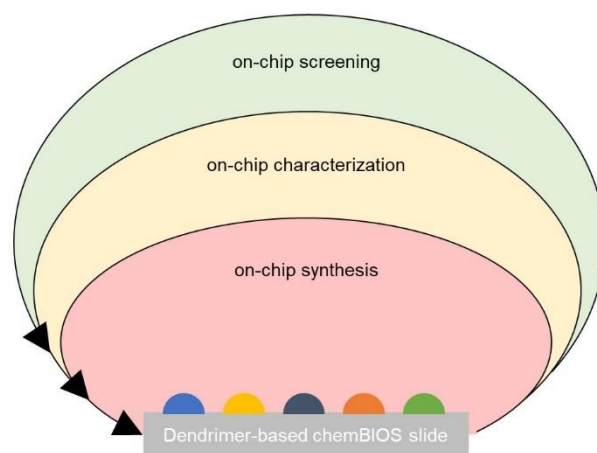




**Supplementary Figure 10 | 3D-printed sandwiching adapter for UV-Vis measurements.** (a-b) Concept art images of a droplet array trapped between two dendrimer-modified, omniphilic-omniphobic patterned slides. The slides were sandwiched using a 3D-printed adapter. (c) Photography of the 3D-printed sandwiching adapter. (d) Schematically showing the top view of the sandwiching adapter with overlaid 384-well microtiter plate patterns. Blue: omniphilic-omniphobic patterned glass slide.



**Supplementary Figure 11 | On-chip cell culture using dendrimer slides.** (a) Schematic diagram showing the process of cell culture and viability tests. Cell suspensions were dispensed to each spot of a dendrimer-based chemBIOS slide and cultured at 37°C under 5% CO<sub>2</sub> for 24 h. Cell staining solution (Hoechst 33342 and propidium iodide) was dispensed to individual droplets and cell viability was evaluated by fluorescence microscopy. (b) Cell viability of on-chip cultured HeLa, HEK293T and Jurkat cells. (c) Microscopy images of stained (Hoechst 33342 and propidium iodide) HeLa, (d) HEK293T, and (e) Jurkat cells. Scale bar: 50  $\mu$ m. Data represent mean  $\pm$  standard deviation; each result based on triplicate control; n=3 independent experiments. Source data are provided as a Source Data file.



**Supplementary Figure 12 | chemBIOS workflow.** Schematic describing the chemBIOS workflow using a dendrimer-modified, omniphilic-omniphobic patterned slide that enables the handling of both low-surface tension liquids (organic solvents) and high-surface tension liquids (aqueous solutions / cell suspension) on the same substrate. On-chip synthesis, on-chip characterization and on-chip screening can be performed using one slide without the need of additional transfer steps.

## Supplementary Tables

**Supplementary Table 1 | Results of contact angle measurements.** N/A: not tested. Each result based on triplicate control; n=3 independent experiments. Source data are provided as a Source Data file.

	solvent	$\theta_{adv}$ [°]	$\sigma_{adv}$ [°]	$\theta_{stat}$ [°]	$\sigma_{stat}$ [°]	$\theta_{rec}$ [°]	$\sigma_{rec}$ [°]
PFDT-modified G3 surface	H <sub>2</sub> O	125	3	116	4	111	3
	DMSO	100	2	97	1	66	2
	DMF	103	1	91	4	67	3
	toluene	89	1	80	2	63	2
	n-hexadecane	86	1	81	2	74	1
	ethanol	80	1	72	2	40	0
Thioglycerol- modified G3 surface	H <sub>2</sub> O	33	2	N/A	N/A	1	1
	DMSO	12	2	N/A	N/A	<1	<1
	DMF	4	1	N/A	N/A	<1	<1
	ethanol	3	1	N/A	N/A	<1	<1

**Supplementary Table 2 | Results of surface roughness (Rq) measurements by AFM.** Each result based on triplicate control; n=3 independent experiments. Source data are provided as a Source Data file.

$\theta(Rq(unmod.))$ [pm]	$\theta(Rq(G0))$ [pm]	$\theta(Rq(G1))$ [pm]	$\theta(Rq(G2))$ [pm]	$\theta(Rq(G3))$ [pm]
212±8	238±23	335±44	424±61	508±26
	$\Delta Rq(G0-unmod.)$ [pm]	$\Delta Rq(G1-G0)$ [pm]	$\Delta Rq(G2-G1)$ [pm]	$\Delta Rq(G3-G2)$ [pm]
	26	97	90	83

**Supplementary Table 3 | Results of dendrimer layer thickness (d) measurements by AFM.** Each result based on triplicate control; n=3 independent experiments. Source data are provided as a Source Data file.

$\theta d(G0)$ [nm]	$\theta d(G1)$ [nm]	$\theta d(G2)$ [nm]	$\theta d(G3)$ [nm]
1.27±0.22	2.03±0.05	2.99±0.19	4.19±0.49
	$\Delta d(G1-G0)$	$\Delta d(G2-G1)$	$\Delta d(G3-G2)$
	0.76	0.95	1.21

**Supplementary Table 4 | Dendrimer layer thickness calculation.**

	<b>bond length [nm]<sup>1, 2</sup></b>
C(sp3)-S	218
S-C(sp3)	218
C(sp3)-C(sp3)	154
C(sp3)-C(sp3)	154
C(sp3)-O	143
O-C(sp2)	143
C(sp2)-C(sp3)	150
C(sp3)-C(sp3)	154
C(sp3)-C(sp2)	150
C(sp2)-C(sp2)	134
Sum	1,618

**Supplementary Table 5 | Mean MALDI-TOF MS Signal-to-Noise (S/N) ratios of lipidoid (L) 1, 2 and 3 measured on 2.83 mm spots before and after on-target washing.** Each result based on triplicate control; n=3 independent experiments. Source data are provided as a Source Data file.

<b>Amount on spot [fmol]</b>	<b>L1 before</b>	<b>L1 after</b>	<b>L2 before</b>	<b>L2 after</b>	<b>L3 before</b>	<b>L3 after</b>
1,000	312±28	956±169	193±11	652±85	367±256	759±192
100	52±10	116±24	35±23	178±89	27±6	150±33
10	4±1	11±1	2±0	10±2	2±0	10±1
2	2±0	3±1		3±0		4±0

**Supplementary Table 6 | Mean MALDI-TOF MS S/N ratios of lipidoid (L) 1, 2 and 3 measured on 900  $\mu\text{m}$  and 500  $\mu\text{m}$  spots after on-target washing.** Each result based on triplicate control; n=3 independent experiments. Source data are provided as a Source Data file.

Amount on spot [fmol]	900 $\mu\text{m}$ spots			500 $\mu\text{m}$ spot		
	L1	L2	L3	L1	L2	L3
1,000	2,601 $\pm$ 274	2,452 $\pm$ 150	2,804 $\pm$ 362	2,666 $\pm$ 141	2,071 $\pm$ 66	2,591 $\pm$ 64
100	1,178 $\pm$ 108	859 $\pm$ 238	767 $\pm$ 221	696 $\pm$ 120	730 $\pm$ 260	818 $\pm$ 75
10	137 $\pm$ 25	65 $\pm$ 15	148 $\pm$ 112	155 $\pm$ 76	338 $\pm$ 264	313 $\pm$ 12
2	47 $\pm$ 21	34 $\pm$ 6	62 $\pm$ 22	35 $\pm$ 7	13 $\pm$ 1	29 $\pm$ 20
0.3	9 $\pm$ 5	4 $\pm$ 1	6 $\pm$ 1	10 $\pm$ 1	8 $\pm$ 3	4 $\pm$ 2
0.1	4 $\pm$ 1	3 $\pm$ 0	3 $\pm$ 0	2 $\pm$ 0	2 $\pm$ 0	3 $\pm$ 2
0.05	3 $\pm$ 0	3 $\pm$ 0		3 $\pm$ 1	1 $\pm$ 0	1 $\pm$ 0

## References

1. Fox, M.A. & Whitesell, J.K. *Organische Chemie: Grundlagen, Mechanismen, Bioorganische Anwendungen*. (Spektrum Akad. Verlag, 1995).
2. Lide, D.R. *CRC Handbook of Chemistry and Physics: A Ready-Reference Book of Chemical and Physical Data*. (CRC-Press, 1984).